

ARTICLE

PREPARATION AND STRUCTURAL PROPERTIES OF POLYANILINE/COTIO3 NANOCOMPOSITES

F Ghanbary*, S Majidi, K Bayzidi, S Khanahmadzadeh

Department of Chemistry, Mahabad Branch, Islamic Azad University, Mahabad, IRAN

ABSTRACT

In this study, poly aniline-cobalt titanate nano composites (NCs) with two content loadings of CoTiO₃ (10 and 20 wt%) were prepared successfully. Fourier-transform infrared spectroscopy (FTIR), X-ray diffraction (XRD), scanning electron microscopy (SEM), energy-dispersive X-ray diffraction (EDX), diffuse reflectance spectroscopy (DRS), and zeta potential were used to characterize the structure and properties of the obtained NCs. The results indicated that CoTiO₃ NPs with an average particle size of 47 nm were distributed in the poly aniline (PANI) matrix; DRS analysis indicated the presence of semiconducting behavior in the NCs. The zeta potential indicated that the fabricated PANI/CoTiO₃NCs with 10 and 20 wt% of CoTiO₃NPs were increased with 83% and 93%, respectively.

INTRODUCTION

As a typical conducting polymer, PANI is one of the most promising electricity-conducting polymers due to its unique electrical and electrochemical properties, easy polymerization, high environmental stability, and the low cost of the monomer [1-3]. The attention PANI has received is attributable to these characteristics and its widespread use in microelectronic devices, diodes, light weight batteries, sensors, and super capacitors. PANI is also used for microwave absorption, inhibition of corrosion, and other related applications [4-8]. The properties of PANI can be tailored by changing its oxidation states and dopants or through blending it with other organic, polymeric, or inorganic nano-sized semiconducting particles to obtain materials with synergistic advantage. Various composites of PANI with inorganic NPs such as CeO₂, TiO₂, ZrO₂, Fe₂O₃, and Fe₃O₄ have been reported. Metal-containing titanium-based oxides such as MTiO₃ (M: Ni, Pb, Fe, Co, Cu, and Zn) are universally known as inorganic functional materials with broad applications. These oxides can be used in a variety of industrial applications including as electrodes of solid oxide fuel cells, metal-air barriers, gas sensors, high-performance catalysts, and ferroelectric random access memory [9-20].

The interest of researchers in CoTiO₃ has increased in recent decades due to its physiochemical properties, which permit its use in applications such as pigments and magnetic recording media, as a gas sensor for alcohol content, and as a humidity sensor [21] and catalyst [22]. Oxide-based magnetic nanoparticles have been investigated by many researchers because of their interesting magnetic properties, including (among others) super-paramagnetic physical properties (mechanical, thermal, etc), which allow polymers to be improved by adding inorganic materials to polymer matrixes; relaxation phenomena; the surface effect caused by their canted spin structure; and magneto-electrical transport. They also have immense potential for applications in the areas of high-density data storage, ferro fluids, magnetic resonance imaging, color processing, and magnetic refrigeration [23]. Super paramagnetic behavior has often been observed in magnetic nanoparticles of dimensions of a few nanometers [24]. In some previous studies, the critical size was estimated to be approximately 30 nm in diameter for a spherical sample of common ferromagnetic materials.

In this study, PANI/CoTiO₃ NCs with two (10, 20 wt%) content loadings of CoTiO₃ were prepared, and the procedure and structural characterization of all PANI/CoTiO₃ NC phases have been investigated using Fourier-transform infrared spectroscopy (FTIR), X-ray diffraction (XRD), scanning electron microscopy (SEM), energy-dispersive X-ray diffraction (EDX), diffuse reflectance spectroscopy (DRS), and zeta potential.

MATERIALS AND METHODS

Cobalt acetate, tetra-n-butyl titanate, stearic acid, potassium iodate, and sulfuric acid were used in the experiments (Merck). The composition of the sample was estimated using EDX attached to a scanning electron microscope at an acceleration voltage of 25 kV (KYKY Model EM 3200; Madell Technology Corporation, Ontario, California, USA). The FTIR spectrum was recorded with a PerkinElmer (Waltham, Massachusetts, USA) Spectrum RX1 using a KBr pellet. The XRD patterns of the powders were recorded on a Seifert Technologies (Massillon, Ohio, USA) diffractometer (Model PTS 3003) using Cu K α radiation ($\lambda=0.15418$ nm) in the range $2\theta=20^\circ$ to 70° to examine the crystallization and structural development of the PANI/CoTiO₃ nano composite. The SEM pictures were recorded with the KYKY Model EM 3200 electron microscope at the previously noted accelerating voltage. DRS patterns of the powders were recorded on a Model Scinco S-4100 (Scinco; Seoul, South Korea). Streaming zeta potential measurements were carried out on a Zeta CAD instrument (France).

KEY WORDS

Nano composite,
CoTiO₃, XRD, EDX, DRS,
zeta potential

Published: 10 October 2016

*Corresponding Author

Email:

Ghanbary83@yahoo.com

Synthesis of CoTiO₃ nanoparticles

CoTiO₃ NPs were prepared through a modified wet-chemistry synthesis method that has been described in the literature [25]. In this procedure, a fixed amount of cobalt acetate was added to the melted stearic acid and dissolved. Stoichiometric tetra-n-butyl titanate was then added to the solution, stirred to form sol, naturally cooled to room temperature, and dried to obtain dried gel. Finally, the gel was calcinated in air at 600 °C to obtain CoTiO₃ NPs.

Synthesis of PANI/CoTiO₃ nano composites

In order to prepare PANI/CoTiO₃ NCs, the essential substances for the preparation of PANI were added (Fig. 1). To prepare PANI, 1 g potassium iodate was added to 100 ml of sulfuric acid (1 M), followed by magnetic mixing to create a uniform solution. After 30 min, the amount of ultra sonicated CoTiO₃ NPs required preparing 10 and 20 wt% of PANI/CoTiO₃ NCs was added to the stirred aqueous solution. After 20 min, 1-ml fresh distilled aniline monomer was also added. Reactions were carried out for 5 h at room temperature. The obtained product was subsequently dried at temperatures of about 60 °C in the oven for 24 h [26]. Finally, PANI/CoTiO₃ NCs were obtained after heat-treatment from 60 °C to 300 °C for 2 h. As described earlier, the entire procedure and structural characterization of PANI/CoTiO₃ NCs phases were investigated using methods including FTIR, XRD, SEM, EDX, DRS, and zeta potential. To overcome this limitation, in this study, poly aniline/CoTiO₃ nano composites were prepared by using a sol-gel synthesis process, as shown in [Fig. 1].

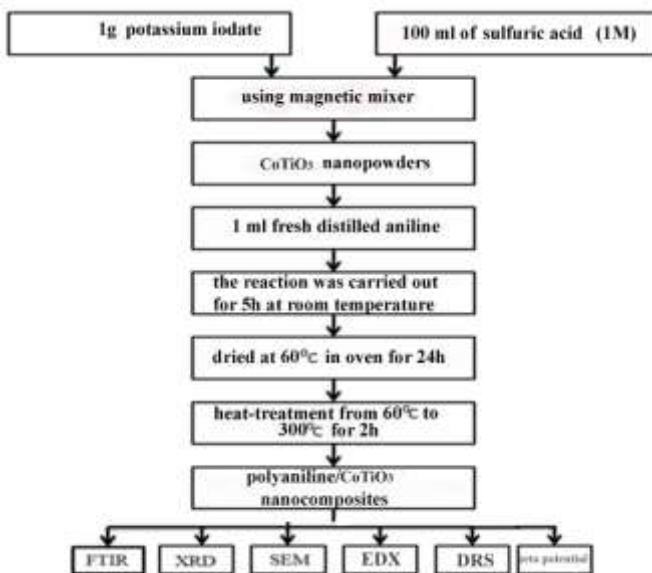


Fig.1: Poly aniline/CoTiO₃ nano composites preparing.

RESULTS AND DISCUSSION

FTIR analysis

[Fig. 1] shows the FTIR spectra of CoTiO₃NPs, pure poly aniline and its NCs with two content loadings (10 and 20 wt%) of CoTiO₃NPs. In [Fig. 2(b)], the absorption peaks at 1480 and 1564 cm⁻¹ correspond to the C=C and C=N stretching modes for the benzenoid and quinoid rings [27]. The peak at 1293 cm⁻¹ is related to the C-N stretching vibration of the benzenoid unit; the band at 799 cm⁻¹ is assigned to out-of-plane C-H bending of the aromatic ring [28]; and, finally, the peak at 1168 cm⁻¹ is attributable to C-N stretching of the secondary aromatic amine [29]. A slight shift in the absorption peaks of composite [Fig. 2(c, d)] is observed compared to PANI and may be due to the interaction between PANI and the surface of the Mn TiO₃NP. The FTIR spectra of the PANI/CoTiO₃NCs, shown in [Fig.1 (c, d)], are almost the same as those of pure PANI. The absorption peaks under the 800 cm⁻¹ are attributed to the vibrations of the Co-O and Ti-O bands in CoTiO₃ NPs [25], a result that indicates the PANI//CoTiO₃ NCs have been synthesized successfully and the observed shift indicates the interaction between PANI and CoTiO₃ NPs.

XRD study

XRD patterns were recorded to analyze the crystal phases. [Fig. 2] shows the XRD patterns of poly aniline, CoTiO₃ NPs, and PANI/CoTiO₃ NCs with different loadings of nanoparticles. The obtained XRD patterns of

CoTiO₃ powders after heat treatment at 600 °C in air for 2 h are shown in Figure 2b. At this temperature, the nano powders displayed sharp and intense peaks, indicating a fine crystalline rhombohedral CoTiO₃ phase. All peaks corresponding to the rhombohedral phase matched well with the database in JCPDS (file number: 77-1373). The XRD pattern of PANI [Fig. 2(a)] shows that PANI has a partly crystalline structure; the two broad peaks are observed at 2θ=20.41° and 25.61° [29]. In [Fig. 2(c-d)], the diffraction peaks at 2θ=20° and 25° correspond to PANI, and the prominent peaks at 2θ=33°, 36°, and 54° correspond to CoTiO₃ nanoparticles. On comparison of XRD patterns of CoTiO₃, PANI, and PANI/CoTiO₃ composites, it is confirmed that CoTiO₃ retained its structure on dispersion in the PANI matrix during the in situ polymerization reaction. The results show that as the CoTiO₃ content increases in 10% and 20% weight fractions, the intensity of the CoTiO₃ crystalline peaks gradually increases. With doping of the PANI matrix with CoTiO₃, the crystal structure of CoTiO₃ was still stable.

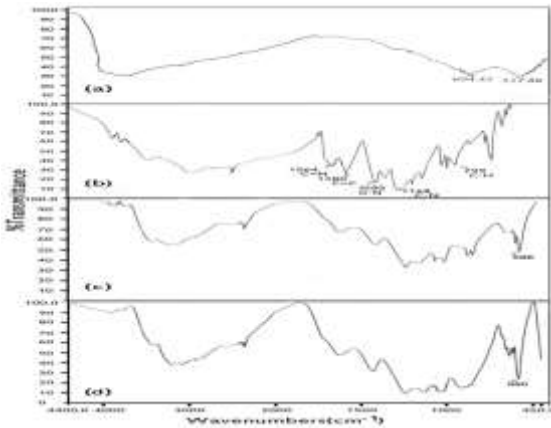


Fig. 1: The FTIR analysis Patterns of the PANI/CoTiO₃NCs.

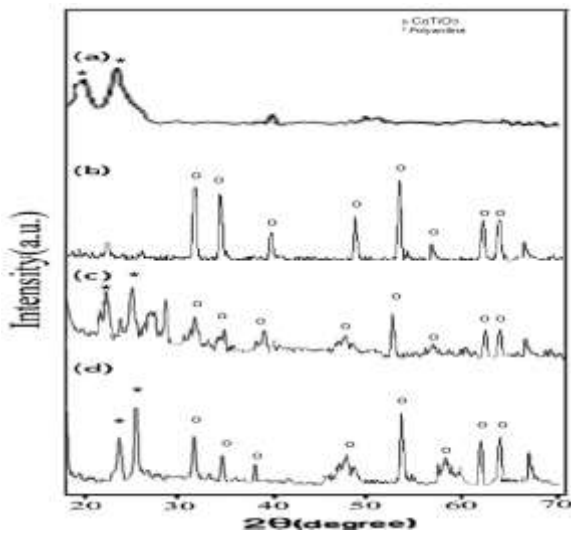


Fig. 2: The XRD Diffraction Patterns of the PANI/CoTiO₃ NCs calcined at (a) 60°C; (b) 100°C, (c) 200 and (d) 300°C.

Morphology of samples

The particle size of powders can be calculated by Scherrer's formula ($t = k\lambda / \beta \cos\theta$), where t is the average size of the particles, assuming particles are spherical, $k=0.9$, λ is the wavelength of radiation, β is the full width at half of the maximum of the diffracted peak, and θ is the angle of diffraction. The particle size was calculated by Scherrer's formula for different calcination temperatures. The crystallite size of the powders calcinated at 600 °C was about 47 nm in diameter, respectively.

$$L = \frac{K \times \lambda}{\Delta(2\theta) \times \cos(\theta)}$$

SEM studies

[Fig. 3] shows the SEM of pure CoTiO₃ [Fig. 3(a)] and the PANI/CoTiO₃ NCs with 10 and 20 wt% of CoTiO₃ NPs loading, respectively [Fig. 3(b-c)]. The particles have an agglomerated grain structure. In the SEM of the NCs, with the increase of CoTiO₃ content, the agglomeration become more appreciable and displayed connections in some regions. SEM images reveal a homogeneous dispersion of CoTiO₃ NPs in the PANI matrix.

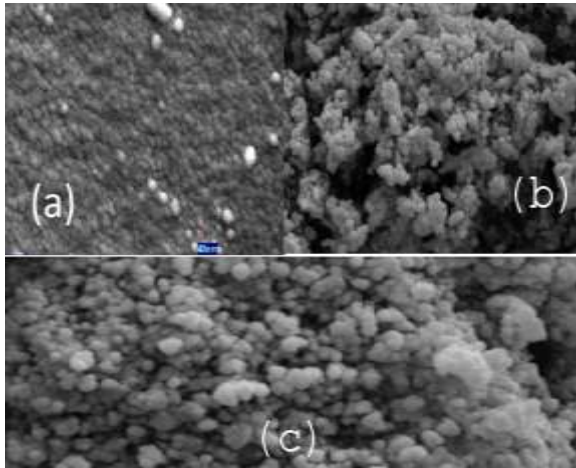


Fig. 3: SEM pictures of PANI/CoTiO₃ NCs.

EDX elemental analysis

EDX patterns of pure CoTiO₃ and the PANI/CoTiO₃ NCs with 10 and 20 wt% loadings of CoTiO₃ NPs are shown in [Fig. 4(a, b)], respectively. EDX patterns of pure CoTiO₃ show separate peaks of cobalt (Co), titanium (Ti), and oxygen; the compositional analysis performed with EDX confirmed that the CoTiO₃ nano powders were obtained. The EDX patterns of PANI/CoTiO₃ NCs with 10 and 20 wt% loadings of CoTiO₃ NPs show separate peaks for cobalt (Co), titanium (Ti), oxygen, carbon, and nitrogen (N), confirming that the sample has the desired composition with both PANI and CoTiO₃ nanoparticles. The results show that the intensity of CoTiO₃ crystalline peaks gradually increases as the CoTiO₃ content increases in the 10 and 20 wt% fractions; this finding is in agreement with the XRD results.

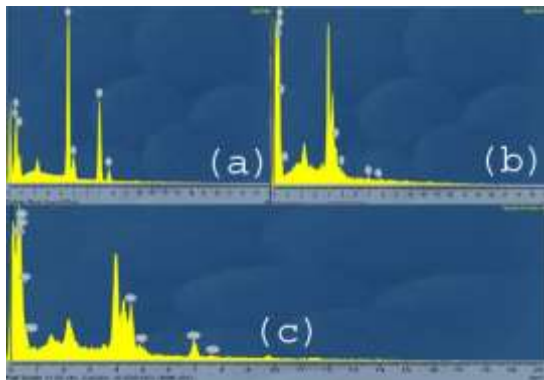


Fig. 4: The EDX pattern of the PANI/CoTiO₃ NCs in Scale Full equal at 1133.

DRS study

The absorption coefficient and optical band gap of a material are two important parameters by which the optical characteristics and its practical applications in various fields are judged. [Fig. 5] shows the DRS of pure CoTiO₃ and the PANI/CoTiO₃ NCs with 10 and 20 wt% fractions of CoTiO₃ NPs loading. In Figure 5a, a sharp absorption peak is observed around 325 nm, indicating the optical band gap attributed to the O²⁻→Ti⁴⁺ charge-transfer interaction [30]. DRS analysis provides information about the semiconducting behavior of the NCs. The value of the direct band gap for PANI/CoTiO₃ NCs with 10 and 20 wt% loadings of CoTiO₃ NPs using the direct band gap determination came out to be 1.4 and 1.3 eV. As a consequence, calculated E_g values

decrease with increasing CoTiO₃ concentration. In the PANI/CoTiO₃NCs with 10 and 20 wt% loadings of CoTiO₃ NPs, sharp absorption peaks are observed around 360 and 365 nm

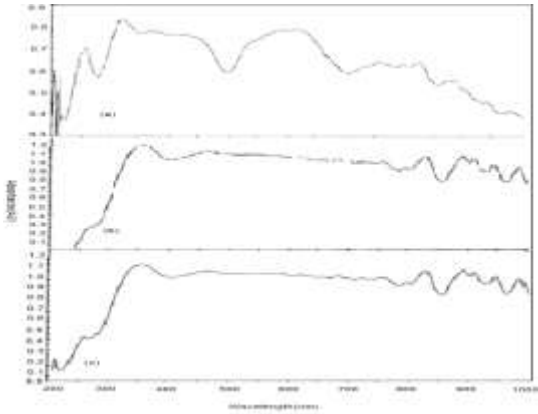


Fig. 5: The DRS chart of PANI/CoTiO₃ NCs.

Band-Gap analysis

For direct band gap determination, a plot of $(\alpha h\nu)^2$ versus $h\nu$ is presented in [Fig. 6]. Band gap value was obtained by extrapolating the straight portion of the graph on the $h\nu$ axis at $(\alpha h\nu)^2 = 0$, as indicated by the solid line in [Fig. 6]. The value of the direct band gap for CoTiO₃ was 2.4 eV; the value is about 2.2 eV for CoTiO₃ bulk crystal, which originates from the $Co^{2+} \rightarrow Ti^{4+}$ charge-transfer transition [31]. The band gap of nano metric CoTiO₃ is higher than that of the bulk crystal, and the energy and shape of the interfacial charge-transfer absorption are expected to change as the size of the particle is reduced to nanometer scale [32–33]; for semiconductors, the energy of the band gap transition increases with decreasing size [34].

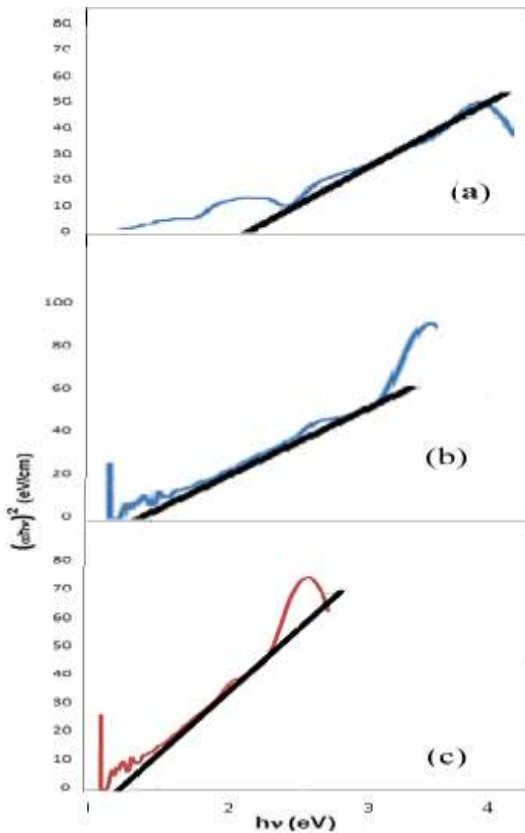


Fig. 6: The band-gap diagram of MgCr₂O₄ nanoparticles.

Zeta potential measurements

[Fig. 7] shows the zeta potential measurements obtained for pure CoTiO₃ [Fig. 7(a)] and the PANI/ CoTiO₃ NCs with 10 and 20 wt% loadings of CoTiO₃ NPs. Initially, CoTiO₃ had an average ζ of 2.27 mV and the PANI/CoTiO₃ NCs with 10 and 20 wt% loadings of CoTiO₃NPs had an average ζ of 25 and 71 mV, respectively. With respect to [Fig. 7], the fabricated PANI/CoTiO₃NCs with 10 and 20 wt% loadings of CoTiO₃NPs were increased with 83% and 93%, respectively.

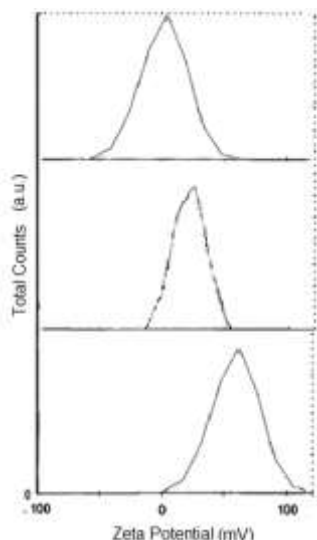


Fig. 7: Shows the zeta potential measurements obtained for pure CoTiO₃.

CONCLUSION

In this study, PANI/CoTiO₃ NCs with two (10, 20 wt%) content loadings of CoTiO₃ were successfully synthesized after heat-treatment from 60°C to 300°C for 2 h. The FTIR study of PANI/CoTiO₃ shows the shift of characteristic absorption bands of the composite due to the interaction of PANI/CoTiO₃. DRS analysis indicates the semiconducting behavior of the NCs; the zeta potential indicated that the fabricated PANI/CoTiO₃ NCs with 10 and 20 wt% loadings of CoTiO₃NPs were increased with 83% and 93%, respectively.

CONFLICT OF INTEREST

There is no conflict of interest.

ACKNOWLEDGEMENTS

The authors would like to thank Islamic Azad University of Mahabad branch for financial supports

FINANCIAL DISCLOSURE

None

REFERENCES

- [1] Majid K, Awasthi S, Singla ML. [2007] Low temperature sensing capability of poly aniline and Mn₃O₄ composite as NTC material. *J Sensor Actuators A*. 135: 113–118.
- [2] Ansari R, Keivani MB. [2006] Poly aniline conducting electro active polymers thermal and environmental stability studies. *E J Chem*. 3: 202–217.
- [3] Jiang J, Ai L, Li LC. [2009] Synthesis and magnetic performance of poly aniline/Mn–Zn ferrite nano composites with intrinsic conductivity. *J Mater. Sci*. 44: 1024–1028.
- [4] Nandi M, Gango padhaya R, Bhaumik A.[2008] Meso porous poly aniline having high conductivity at room temperature. *Micropor. Mesopor. Mater*. 109: 239–247.
- [5] Zhao C, Xing S, Yu Y, Zhang W, Wang C. [2007] A novel all-plastic diode based upon pure poly aniline. *Micro electron*. 38: 316–320.
- [6] Dalas E, Vitoratos E, Sakkopoulos S, Malkaj P. [2004] Poly aniline/zeolite as a cathode in a novel gel electrolyte primary dry cell. *J Power Sources*, 128: 319–325.
- [7] Ryu KS, Lee Y, Han KS, Park YJ, Kang MG, Park NG, Chang SH. [2004] Electrochemical super capacitor based on poly aniline doped with lithium salt and active carbon electrodes. *Solid State Ionics*. 175: 765–768.
- [8] Manigandan S, Jain A, Majumder S, Ganguly S, Kargupta K. [2008] Formation of nano-rods and nano-particles of poly aniline using Langmuir Blodgett technique: performance study for ammonia sensor. *Sensor Actuators B*. 133: 187–194.
- [9] Yamamoto O, Takeda Y, Kanno R, Noda M. [1987] Perovskite-type oxides as oxygen electrodes for high temperature oxide fuel cells. *Solid State Ion*. 22: 241–246.

- [10] Phani AR, Santucci S. [2001] Structural characterization of nickel titanium oxide synthesized by sol-gel spin-coating technique. *Mater. Lett.* 50(4): 240-245.
- [11] Fisch R. [1995] Critical behavior of randomly pinned spin-density waves. *Phys. Rev. B.*, 51(17): 11507-11514.
- [12] Shimizu Y, Uemura K, Miura N, Yamzoe N. [1988] Gas-diffusion electrodes for oxygen reduction loaded with large surface area $\text{La}_{1-x}\text{Ca}_x\text{MO}_3$ (M=Co,Mn). *Chem. Lett.* 67: 1979-1982.
- [13] Harris QJ, Feng Q, Lee YSB, Rigeneau RJ. [1997] Random fields and random anisotropies in the mixed Ising-XY magnet $\text{Fe}_x\text{Co}_{1-x}\text{TiO}_3$. *Phys. Rev. Lett.* 78: 346-349.
- [14] Taylor DJ, Fleig PF, Page RA. [2002] Characterization of nickel titanate synthesized by sol-gel Processing. *Thin Solid Films.* 408: 104-110.
- [15] Obayashi H, Sakurai Y, Gejo T. [1976] Perovskite-type oxides as ethanol sensors. *J. Solid State Chem.* 17: 299-303.
- [16] Dharmaraj N, Park HC, Kim CK, Kim HY, Lee DR. [2004] Nickel titanate nano fibers by Electro spinning. *Mater. Chem. Phys.* 87: 5-9.
- [17] Skoglundh M, Lowedahl L, Janson K, Dahl L, Nygren M. [1994] Characterization and catalytic properties of perovskites with nominal compositions $\text{La}_{1-x}\text{Sr}_x\text{Al}_{1-2y}\text{Cu}_y\text{Ru}_y\text{O}_3$. *Appl. Catal. B.* 3: 259-274.
- [18] Liu H, Wang B, Wang R, Liu X. [2007] Preparation and electric characteristics of gadolinium substitute bismuth titanate ferroelectric thin films. *Mater. Lett.* 61(11-12): 2457-2459.
- [19] Wang DG, Chen CZ, Ma Jd, Liu TH. [2008] Lead-based titanate ferroelectric thin films fabricated by a sol-gel technique. *Appl. Surf. Sci.* 255(5): 1637-1645.
- [20] Bobby Singh S, Sharma HB, Sarmaa HNK, Phanjobama S. [2008] Influence of crystallization on the spectral features of nano-sized ferroelectric barium strontium titanate ($\text{Ba}_{0.7}\text{Sr}_{0.3}\text{TiO}_3$) thin films. *Physica. B: Condens. Matter.* 403(17): 2678-2683.
- [21] Chu X, Liu X, Wang G, Meng G. [1999] Preparation and gas-sensing properties of nano- CoTiO_3 . *Mater. Res. Bull.* 34(10-11): 1789-1795.
- [22] Kazuyuki T, Yasuo U, Shuji T, Takashi I, Akifumi U. [1984] Catalyst preparation procedure probed by EXAFS spectroscopy: 2. Cobalt on titania. *J. Am. Chem. Soc.* 106: 5172-5178.
- [23] Sahoo Y, Cheon M, Wang S, Luo H, Furlani EP, Prasad PN. [2004] Field-directed self-assembly of magnetic nano particles. *J Phys Chem B.* 108(11): 3380-3383.
- [24] Enhessari M, Parviz A, Ozaee K, Karamali E. [2010] Magnetic properties and heat capacity of CoTiO_3 nano powders prepared by stearic acid gel method. *J Exp Nano sci.* 5(1): 61-68.
- [25] Enhessari M, Parviz A, Karamali E, Ozaee K. [2012] Synthesis, characterisation and optical properties of MnTiO_3 nano powders. *J Exp. Nano sci.* 7(3): 327-335.
- [26] Mansour MS, Ossman ME, Farag HA. [2011] Removal of Cd (II) ion from waste water by adsorption onto poly aniline coated on sawdust. *Desalination.* 272: 301-305.
- [27] Zhu J, Wei S, Zhang L, Mao Y, Ryu J, Karki AB, Young DP, Guo Z. [2011] Poly aniline tungsten oxide meta composites with tunable electronic properties. *J Mater. Chem.* 21: 342-348.
- [28] Gu H, Huang Y, Zhang X, Wang Q, Zhu J, Shao L, Haldolaarachchige N, Young DP, Wei S, Guo Z. [2012] Magneto resistive poly aniline-magnetite nano composites with negative dielectric properties. *Polymer.* 53: 801-809.
- [29] Umarea SS, Shambharkara BH, Ningthoujam RS. [2010] Synthesis and characterization of PANI- Fe_3O_4 nanocomposite: Electrical conductivity, magnetic, electrochemical studies. *Synth. Met.*, 160: 1815-1821.
- [30] Zhou GW, Chen DR, Xu GY. [2005] Synthesis and characterization of ilmenite-type CoTiO_3 Nano materials. *ActaChim. Sinica.* 20: 1971-1920.
- [31] Kao KH, Chuang SH, Wu WC, et al. [2008] X-ray photoelectron spectroscopy energy band alignment of spin-on CoTiO_3 high-k dielectric prepared by sol-gel spin coating method. *Applied Physics Letters.* 93: 092907-092907-2.
- [32] Creutz C, Brunschwig BS, Sutin N. [2004] Electron transfer from the molecular to the nano scale, in *Comprehensive Coordination Chemistry II*. J McLeverty and T. J Meyer, eds. 7: 731-777.
- [33] Jortner J. [1992] Cluster size effects. *Z. Phys. D At. Mol. Clusters.* 24(3): 247-275.
- [34] Hagfeldt A, Gratzel M. [1995] Light-induced redox reactions in nano crystalline systems. *Chem. Rev.* 95(1):49-68.